# Overcoming the operational challenges encountered during a decade of conjunctions

**Mark A. Vincent**
*Raytheon Intelligence and Space*

## ABSTRACT

Operational challenges remain in assessing satellite conjunctions and determining Risk Mitigation Maneuvers (RMMs). This paper will analyze the trade-offs between the time it takes to generate Maneuver Trade Space plots and their accuracy. The extent of the computer run time is dominated by the models used to propagate the primary object backwards from the Time of Closest Approach (TCA) to the time of a potential RMM and then forwards to the new TCA. Comparisons are made from using different sized gravity fields and osculating Cartesian versus Mean equinoctial elements. Other operational issues involve the aggregate risk from multiple secondary objects.

## 1. INTRODUCTION

The operational processes used to address the risk of objects colliding in space started from early considerations for the International Space Station. In particular Foster and Estes [1] created the framework for the Probability of Collision (Pc) being measured in the two-dimensional conjunction plane. The assumptions inherent in this formulization are valid for most conjunctions. More recently, a three-dimensional method [2] was developed to produce good results for the cases that the 2-D method was not sufficient. Results from Monte Carlo and other sampling techniques were used as standards to test the analytical methods. Even though these sampling methods used less "draws" or "sigma points" than a doing a full-factorial representation, it was still computer-time-intensive to propagate six- or higher dimension covariance matrices with high-fidelity force models. Studying these modeling and runtime burdens are analogous to the analysis performed for this paper regarding Maneuver Trade Space (MTS) plots, as explained in the following sections.

## 2. CONOPS AND TOOLS OF THE TRADE

The USAF 18$^{th}$ Space Squadron screens all active missions versus the catalogue nominally three times per day. Conjunction Data Messages (CDMs) are created for conjunctions that occur in corresponding Monitor Volumes (e.g. a +/-2 km radial, +/-25 km in-track and +/-25 km cross-track ellipsoid for the LEO missions discussed in this paper). The CDMs for NASA missions are used to produce Summary Reports created both by the Conjunction Assessment and Risk Analysis (CARA) Orbit Specialist Analysists at Vandenberg Air Force Base and separately by the CARA team at GSFC (plus commercial companies). A new process at the Jet Propulsion Laboratory (JPL) is also now sending out similar reports. These reports contain warnings, in particular a "red event" is the Pc exceeds the commonly-accepted maneuver threshold of $1x10^{-4}$. Miss components, usually in radial, in-track and cross-track are also provided and were used extensively for decision making before Pc thresholds became the metric of choice. Briefly, the switch to using Pc was done because even small miss distances can imply a low likelihood of a collision if the uncertainty in the satellites relative positions is high, though the discussion on this subject continues, albeit not in this paper, at least not explicitly.

Instead, the focus here will be on how tools such as the MTS plots can aid in the planning and decision making processes that start 3 or 4 days before the Time of Closest Approach (TCA) of the conjunction and with a go or no-go decision for a Risk Mitigation Maneuver (RMM). Nominally this decision occurs at a mission telecon meeting, although sometimes the decision made at that time can be contingent on new reports coming in, perhaps containing a new tracking solution for the secondary object of interest that happens in the middle of the night. Compounding the time-sensitivity of the process is the natural behavior of the Pc as new tracking data is obtained and the predicted covariance at TCA of the two objects is reduced, mainly due to the shorter propagation time involved. As discussed extensively [3] the tendency for Pc to start low, reach a maximum and then decrease implies a great advantage in waiting to make the RMM decision until the last practical epoch. Therefore, a rapid turnaround from getting the CDM data and producing an MTS plot to pick the proper RMM magnitude and direction can be crucial. Another advantage of producing MTS plots quickly is for parametric studies, especially when the Pc is over a mission's planning threshold (say 2 or 3 $x10^{-5}$) but below their maneuver execution threshold of $1x10^{-4}$.

## 3. MANEUVER TRADE SPACE PLOTS

MTS plots are invaluable tool for choosing what mitigation action should be performed for a single conjunction or with multiple conjunctions with the same secondary object or a number of secondaries. Fig. 1 depicts the usual choice of axes. The bottom of the y-axis represents the Time of Closet Approach (TCA) with the main secondary of interest, correspondingly the y-axis represents the time before this epoch when a Risk Mitigation Maneuver (RMM) may be performed. The x-axis represents the choice of the magnitude of the RMM and in most practical applications it represents an In-track maneuver, negative representing a retrograde maneuver and positive representing a posigrade maneuver. Note, here "in-track" means perpendicular to the radial direction which is a common maneuver direction choice for near-circular satellites, though a few missions actually burn in the velocity direction. The important point being that the MTS plot should match how the spacecraft is potentially going to maneuver. The color contours are the resulting Pc from preforming the maneuver. The dashed line represents the new (maximum) post-RMM threshold dictated by CARA.

Data from the Orbiting Carbon Observatory-2 (OCO-2) mission will be used throughout this paper. It flies in a frozen, sun-synchronous orbit with an equatorial altitude of 705 km with a ground track repeat of 16 days and 233 revolutions. This corresponds to a nominal orbital period just under 99 minutes. Thus the optimal "blue peninsulas" in Fig. 1 correspond to doing the RMM 180 degrees in argument of latitude (aol) from the conjunction because that gives the maximum radial separation from the secondary object. In the early days of conjunction assessment, consideration was given for doing an early along-track maneuver so the along-track separation at the conjunction was increased. However, for most missions it is better to wait and rely on a radial separation (though as the fourth figure of [4] indicates, in half of the possible geometries, using both radial and along-track increases in separation is possible). It is also worth noting that although not commonly used, doing a radial maneuver does have an advantage. Do such a maneuver 90 degrees away from a conjunction also increases the radial separation while not changing the orbital period of the Primary object. This can be advantageous when a mission has a tight orbital tube or diamond to fly in [5]. The disadvantages include requiring twice the maneuver magnitude for the same radial change, and no change in along-track separation in the situation that that would be advantageous. These disadvantages are evident in Fig. 2 where the Pc from radial burns are less than 50% effective compared to In-track burns. Note in this figure the range of burn magnitudes is twice as large as other figures in this paper in order to give a better comparison.

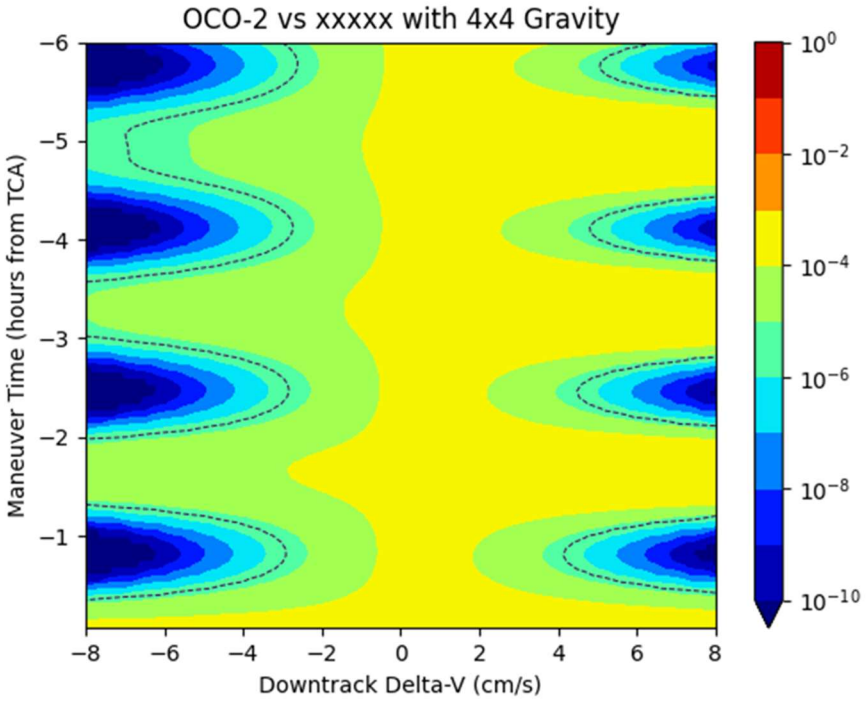


Fig. 1. Example of a Maneuver Trade Space Plot

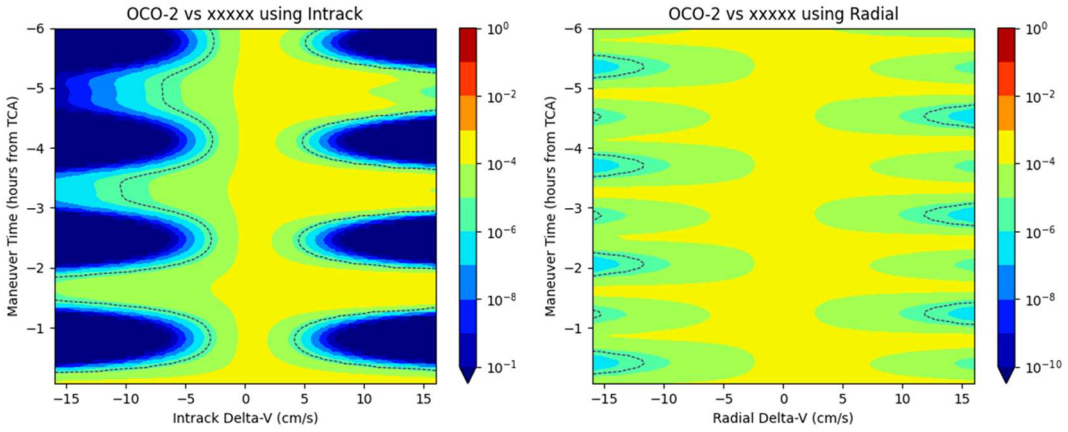


Figure 2. Comparing In-track and Radial RMMs

In order to introduce the improvements to the MTS plot generation described in this paper, it is best to first characterize the steps required to make the plot. As described above, the CDM message provides the state and covariance for the Primary and Secondary bodies for a given conjunction at the TCA epoch. The state consists of Cartesian elements in the International Terrestrial Reference Frame (ITRF) while the covariance is in Cartesian elements in the local Radial, In-track, Cross-track (RIC) frame. The process of rotating the state and covariance and projecting them onto the Conjunction Plane was first credited to Foster and Estes [1] and is well documented elsewhere in the literature, for a good graphical representation see [6]. The salient point being this is all done in Cartesian elements, though attempts have been made to do otherwise [7].

Fig. 3 depicts the process for generating data used in the MTS plot. The Primary object state is propagated backwards in time to a series of possible RMM times and for each possible maneuver time, another series represents the possible maneuver sizes (the range of times and maneuver sizes being user choices). The maneuver is "applied" and then the new Primary body state is propagated back to the original TCA where a search is performed to find the new TCA. The Secondary object state is the propagated to this new TCA (note the difference in TCA times is usually of the order of a second or two) and then the new Pc value is calculated.

The extreme method of doing the above process would be to do the Primary (and Secondary) object propagations with a Cowell-like integration with all available force models included. Since the Primary body state is kept in Cartesian elements, the maneuver can simply be applied to the velocity components, albeit with a state rotation to RIC from an inertial coordinate system such as EME2000 (Earth Mean Equator of 2000) and back again. However, as will be described below this can be prohibitively slow in computer run time and not be necessary for the required accuracy for the MTS plot. These improvements were done in three phases, reduced force modelling, Mean elements and alternative Mean element/maneuver methods.

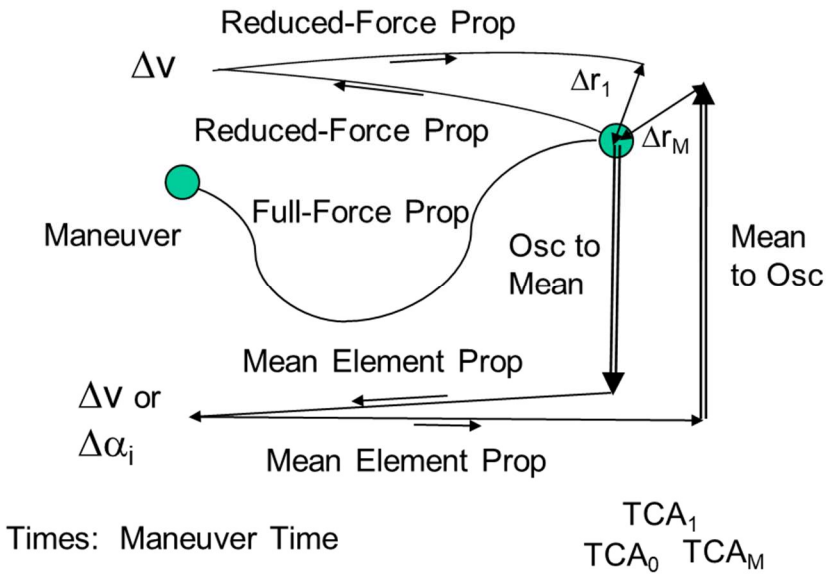


Fig. 3: Alternative Methods for Propagations

### 3.1 Reduced Force Model and Gravity Field Comparisons

The basic concept underlying this sub-section and to some extent the following sub-sections is that although the propagation backwards from TCA to maneuver time with a limited model may end up with a state that deviates from the "truth" (here truth can be thought of as the high fidelity force model), when the propagation occurs back to the new TCA the errors in the final state have been cancelled to a large extent. This subject is analogous or identical to the non-linearities involved in propagating the state transition matrix [8]. It can also be thought of in the context of the accuracy of difference in the Osculating/Mean conversions at the two time epochs (assuming the Mean element propagation in between can be done quickly and accurately), as will be presented in the following two sub-sections.

Even for the Osculating element propagation method, insight can be gathered by studying the underlying Mean elements involved. Consider using just a two-body method for propagating back and forth. This scenario implies that the five Osculating elements (excluding the true anomaly or equivalent) at TCA are considered to be fixed. Thus at the maneuver time ($T_{RMM}$) there is a new set of Osculating elements consisting of the original five elements and the corresponding new true anomaly. However, except for the particular case of being at the same geographical location, the Osculating elements at $T_{RMM}$ correspond to a different set of Mean elements than those at TCA. Note that this difference is the same amount that the Osculating elements vary about the Mean elements around the orbit, for example, up to 8 km in semi-major axis for LEO satellites.

A common rule-of-thumb is that a Δv can be applied to either Mean or Osculating elements with equivalent results. To evaluate this assumption a semi-analytical analysis was performed. In the future a pure analytical approach might be possible at least to order $J_2$ in the gravity field. Some initial observations are that the Osculating and Mean elements both correspond to Keplerian ellipses. The Mean semi-major axis is the average of the Osculating semi-major axis. However, the Mean radius is not the average of the Osculating radius. In fact, for most definitions of Mean elements, the Mean radius is always less than the Osculating value for a given aol, (see the first figure of [7]).

To see how the semi-major axis and radius differences affect the change of semi-major axis, differentiate and re-arrange the vis-viva equation to get:

$$\Delta a = \frac{2a^2}{\sqrt{\mu}} \sqrt{\left(\frac{2}{\mathrm{r}} - \frac{1}{a}\right)}\, \Delta \mathrm{v}$$

showing how $\Delta a$ is a function of $a$ and $r$. Therefore, in the previous example the effect of the $\Delta a$ is in general different at $T_{RMM}$ than it is at TCA or a different maneuver time. To understand this further a time series of the Osculating and Mean values for the A-Train reference orbit were used to calculate the radius and along with the semi-major were plugged into the formula above to calculate $\Delta a$ for a $\Delta v$ = 5 cm/s and presented in Fig. 3.

Since the curves in Fig. 4 start at the descending node and the period of the OCO-2 orbit is just under 100 minutes and it is a near-circular (i.e. frozen) orbit, implies that near 25 minutes is the apogee and near 75 minutes is the perigee. The Mean curve then exhibits the commonly known fact that it is more efficient to burn at perigee than apogee. The behavior of the Osculating curve is more complex, partly because as explained in [7], the minimum radius happens at an Osculating apogee, at least for this type of orbit. And the salient point for the above discussion about propagation methods is that the $\Delta a$ applied to Osculating vs. Mean elements is only equivalent at 4 points along the orbit. The black square and circle are explained in Section 3.3.1.

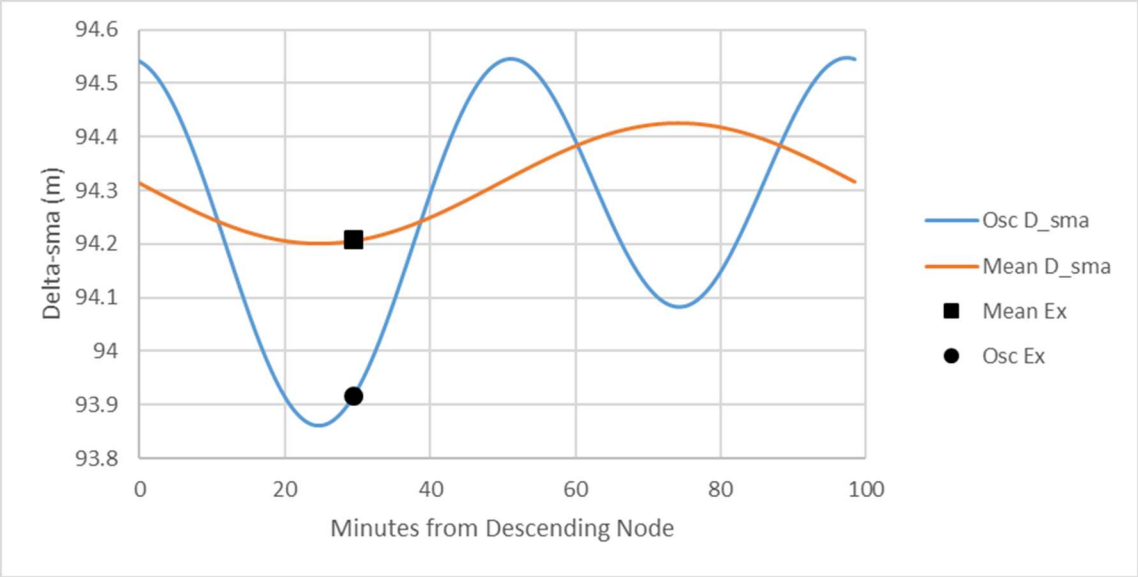


Fig. 4 Mean and Osculating Delta-sma for a 5 cm/s Along-track Delta-velocity

A preliminary numerical test compared the results from using a series of force models to the standard values produced from the Full-force model contained in the "lockfile" for the NISAR mission. The lockfile contained models for a 360x360 gravity field, atmospheric drag and solar/albedo radiation pressure. This test just compared the positional difference from propagating back and forth. In Table 1 the results in the Radial, Transverse, Normal (RTN, which is the same as the RIC system discussed later) coordinates is more informative. As expected the effect was largest in the transverse direction, medium for normal and smallest for the radial direction. However, as an additional preliminary analysis, the Pc change for +/- 10 m variations in the RTN directions confirmed that the Pc sensitivity was opposite, largest for radial, medium for normal and smallest for transverse directions.

A further point should be made from continuing the above discussion regarding the Mean element orbits. Using the same logic, omitting drag, for example, in the propagations will cause the semi-major axis to be different at TRMM (both directly and because of the along-track difference) but this will be of the order of meters rather than the kilometers corresponding to $J_2$. This is the justification for leaving out all the non-gravity terms in the propagations in the MTS comparisons. This conclusion is supported by the fact that the results for the 20x20 gravity (only) case in Table 1 has a very small difference with respect to the Full model. Nevertheless, further investigation was done to verify and quantify the effects of the non-gravitational forces by comparing gravity-only, gravity + drag and the full model. Since the difference between the first and last cases was only a matter of millimeters, the contribution from the drag was hard to distinguish with perhaps the only conclusion being that the other non-gravitational terms were just as important as the drag and the overall assumption that gravity-only could be used was confirmed. Plus, it is worth noting that adding the drag tripled the computer run time and the good results for the 4x4 case in Table 1 are relevant to the investigation described next.

**Table 1. End-point Deviations for a 5 cm/s RMM and a 12-hour Propagation**

| Model | Run Time (sec) | ΔX or ΔR (m) | ΔY or ΔT (m) | ΔZ or ΔN (m) |
|---|---|---|---|---|
| FULL | 7.21 | | | |
| 2body: | <0.01 | 6.429 | -1.045 | -8.324 |
| in RTN | | 0.415 | 10.489 | -1.236 |
| STM : | <0.01 | -2.550 | -0.806 | -1.479 |
| in RTN | | -3.051 | -0.188 | 0.001 |
| J2-only | 0.09 | 0.184 | 0.028 | -0.282 |
| in RTN | | 0.003 | 0.337 | 0.027 |
| 2x2 | 0.09 | 0.095 | 0.020 | -0.151 |
| 4x4 | 0.09 | 0.004 | 0.013 | -0.001 |
| 6x6 | 0.11 | 0.038 | 0.012 | -0.028 |
| 10x10 | 0.17 | -0.005 | 0.006 | 0.022 |
| 20x20 | 0.26 | -0.003 | -0.002 | 0.000 |

With these preliminary conclusions in hand, the focus turned to the main analysis, that is, how much does the size of the gravity field affect the generation of the MTS plots. Fig. 5 contains the results for runs using Two-body, J2-only, and degree x order: 2x2, 4x4, 8x8, 12x12, 16x16, 20x20, 24x24, 28x28, 32x32, 36x36 and 40x40 gravity fields. The x axis represents the degree index in the non-two-body fields, that is, x = 0 represents 2x0, x = 2 represents 2x2, etc. The blue curve (and left y-axis) represents the maximum amount the Pc in the MTS plot (see Fig. 4) differed from the next-sized-smallest gravity field. Thus leftmost blue dot represents how much 2x0 results differed from the Two-body results, the next blue dot to the right how much the 2x2 results differed from the 2x0 results, etc. The green dashed line (and right y-axis) represents the computer run time in wall clock units which in this case was a good proxy for the CPU used. The Two-body run time was about 18 seconds. Note these runs did not use the parallelization that was available on the JPL nexus cluster of computers. The horizontal line is the (no RMM) Pc value of $1.389 \times 10^{-4}$ but just used as a reference since, of course, the Pc varies across the extent of all the MTS plots.

The results are typical for analyzing the effect of gravity field terms. The effect of the dominant $J_2$ term is much larger than the other 2x2 terms, though its moderate contribution ($2.86 \times 10^{-5}$) indicates that the Two-body effect by itself is not that bad for representing the higher gravity fields. The 4x4 through 8x8 terms have about the same effect and then the influences of the higher terms tend to decrease with perhaps near resonances with the 16x16 and 32x32 terms (corresponding to the aforementioned OCO-2 16-day, 233-rev repeat ground track).

The time taken for each run increases in a linear or quadratic fashion keeping in mind that the number of terms for a n x n field is $n^2 + 2n - 3$ (which is easily calculating by combining the formula Gauss calculated during his "hall detention" plus the fact that there are no degree 1 gravity terms due to the choice of the origin). Picking an acceptable run time is dependent on the user's application (and patience) but the 4x4 value appears to be a "knee in the curve."

For the JPL report process there will be a low-fidelity screening to determine which of the conjuncting secondary objects should be included over the ranges of possible maneuver magnitude and times of the MTS plot. The Two-body gravity model should be sufficient to do this screening. For the follow-on high-fidelity Aggregate Pc MTS plot (see Section 4), the 4x4 model should suffice, with perhaps using a higher gravity field if parallelization is utilized.

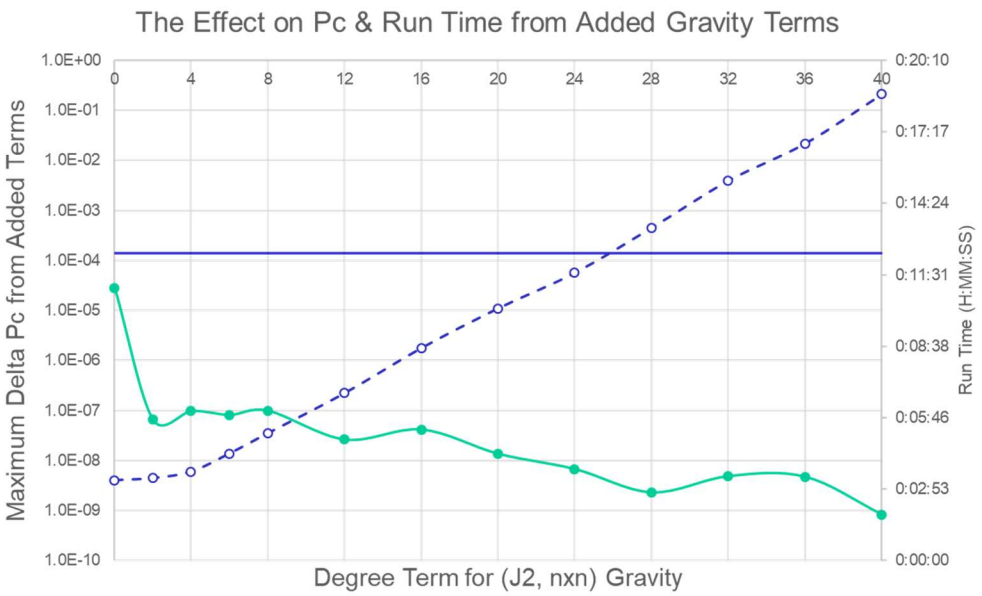


Fig. 5: Comparing the Contribution to Pc and Run-times from Gravity Field Terms

To further understand the differences between using different sized gravity field, consider Fig. 6. It corresponds to the same conjunction and MTS plot parameters as Fig. 1. Thus, where the Pc difference is rather large, the absolute value of Pc is also large (though *vice versa*, large absolute Pc values implying large differences is only true part of the time). Also, although the larger differences, say greater than $1x10^{-5}$, appear to be significant compared to the maximal absolute values seen to be in the $10^{-4}$ range in Fig. 1, most RMM maneuvers occur in the two hours preceding TCA and are 5 cm/s or less. Nevertheless, the previous conclusion that a 4x4 gravity field provides a significant improvement over a two-body model is still valid (albeit the $J_2$ term contributed the most).

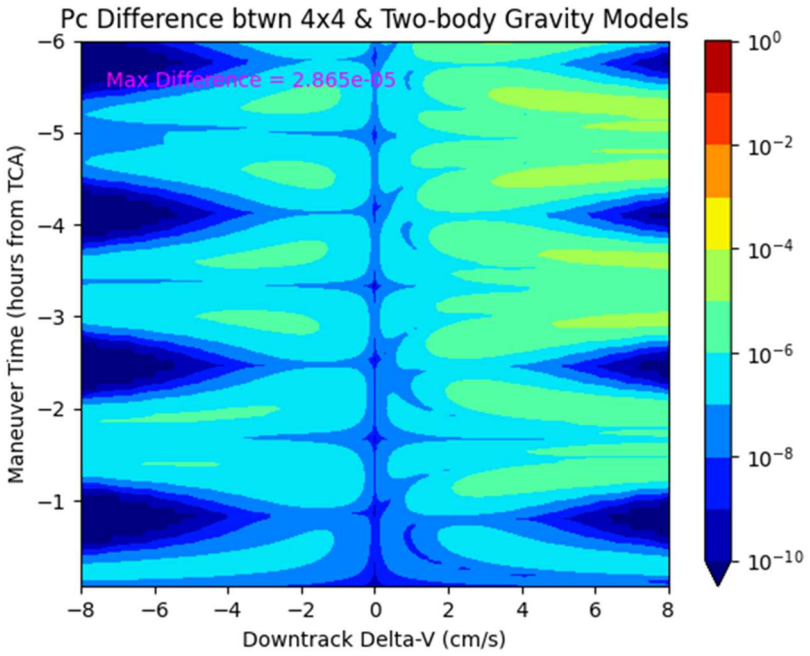


Fig. 6: Alternative Methods for Pc Differences between 4x4 and Two-body Gravity Fields

As a final comparison consider Fig. 7 which depicts the difference between a 40x40 and 4x4 gravity fields. Thus is represent the cumulative effect of the blue dots of Fig 5., excluding the three leftmost dots whose effect is represented in Fig. 6. However, the areas of higher of Pc differences are still roughly in the same regions of Figs. 6 and 7.

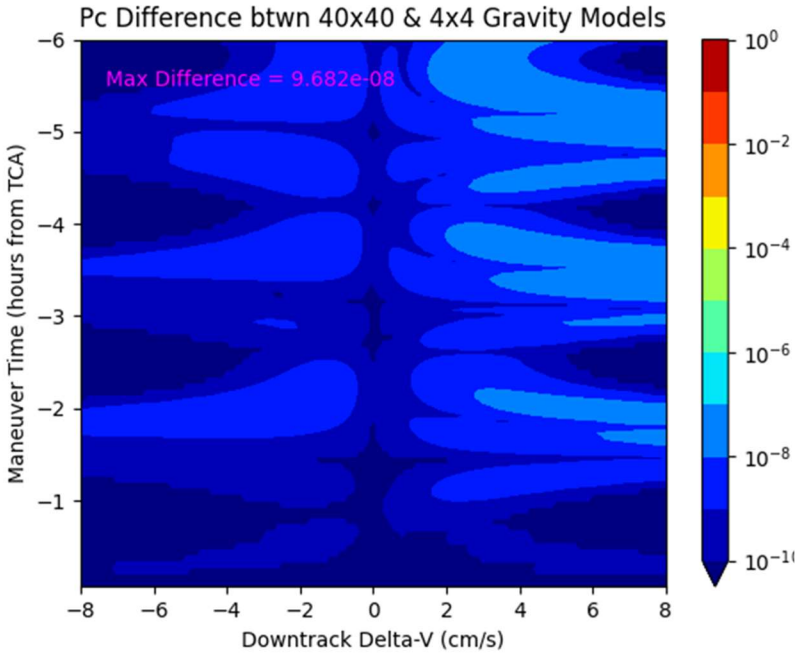


Fig. 7: Pc Differences between 40x40 and 4x4 Gravity Fields

### 3.2 Mean Element Propagations

There is a long history of Mean elements usage at JPL. The Long-term Orbit Predictor (LOP) was produced by Kwok [9] in the 1980's which performed a semi-analytical propagation of Mean elements but had only had a $J_2$ conversion between Mean and Osculating input/output elements. The $J_2^2$ terms were added into a later program named POLOP which became part of the Planetary Observer Planning Software [10]. Note that POLOP was very useful for doing orbit lifetime studies since it runs about 1000 times faster than the equivalent Cowell-like integration of Osculating elements. For Mean/Osculating conversions using a full gravity field a separate program named OSMEAN [11] was created using Kaula's theory [12].

Ely created a numerical version of both the conversion and propagation algorithms and originally called it Morbiter, [13, 14] though now it is built into the MONTE (Mission analysis, Operations, and Navigation Toolkit Environment) software suite at JPL. These formulizations were used in the implementation described in the next subsection, though alternative methods are presented in the subsection 3.3.

### 3.3 Implementation of Mean Elements into the MTS Generation Process

Although the benefit of doing propagations with Mean elements is clear, there are some complications when implementing them into the overall process of generating an MTS plot, as seen in Fig. 8. The steps above the dashed lines and no-burn "projection onto the Conjunction Plane and calculate Pc" are all part of the standard 2-D Pc calculation. Plus, the conversion of the Primary body state from Osculating to Mean and propagating backwards from (the original) TCA are straightforward. Applying the delta-v can be done in a variety of ways and is discussed in sub-section 3.3.1. In all cases there is a post-maneuver set of Mean elements that are then propagated forward to a time just beyond the original TCA. This "time beyond" only has to be a couple of seconds since the new TCA will

be close to the old value, noting however that with a relative speed of order 10 km/s, fractions of a second imply significant changes in Pc. Fortunately, the motion of the two bodies during this delta-TCA can be considered near linear (noting that one of the assumptions of the 2-D Pc method is linear relative motion during the conjunction). Thus for the Primary body, five points were chosen centered on the old TCA (i.e. TCA-2, TCA-1, TCA, TCA+1, TCA+2 seconds) and converted to Osculating. A 5-point Lagrangian spline can be fit to these Osculating points. For the Secondary body a simple trajectory can be created by using the original Osculating elements and a two-body propagation during the TCA +/- 2 second search region. With trajectories for both bodies in hand, a simple one-dimensional search routine can be used to find the closest separation. Nevertheless, the efficiency of the Mean element propagation has been diluted by having to do a number of conversions for every point in the MTS plot, the subject of the next two subsections.

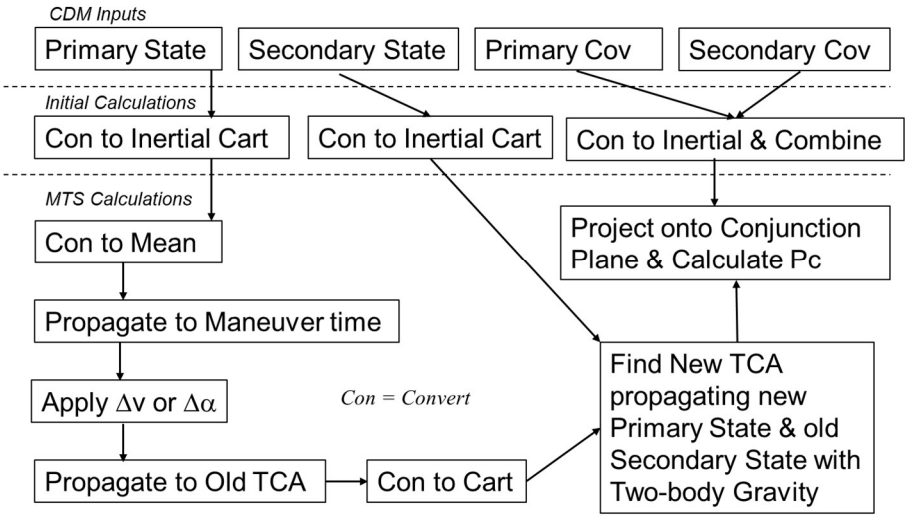


Fig. 8: Flowchart for Implementing Mean elements into MTS Plot Generation

### 3.3.1 Comparison of applying the delta-v to different orbital elements

In the "Apply Δv or Δα" box in Fig. 8 there is a choice of two methods of applying the Δv (using the Δα is discussed in Subsection 3.4.1). The more accurate method is to convert the Mean elements to Osculating elements, then convert to Cartesian elements and alter the velocity components, then convert back to Osculating orbital elements and finally convert back to Mean elements. The "shortcut method" avoids the conversions to and from Osculating and only does the convert to Cartesian elements, apply the Δv, convert to Mean elements steps. The following presents the results from an investigation into the error accumulation from using the shortcut method.

A 5 cm/s RMM was applied 50 minutes (about ½ an orbit) before an actual OCO-2 conjunction. The Osculating initial conditions were converted to Mean at TCA and then propagated back to the maneuver time and then the Δv was applied in the two manners described above and the results are presented in Table 2.

**Table 2. Comparing methods to apply the delta-velocity**

| Result | Description of Delta Semi-major Axis of Interest | Value (m) |
|---|---|---|
| 1 | Mean sma using Shortcut Method | 94.210 |
| 2 | Mean sma using Full Method | 94.171 |
| 3 | Osculating sma inside Full Method | 93.917 |
| 4 | Mean sma using Full Method & Mean velocity direction | 94.171 |

The main difference of interest, Results 1 and 2 is just over 5 cm. Since the propagation time back to the (old) TCA is 50 minutes, this corresponds to an along-track difference just under 38 cm (or if it were 1.5 orbits instead, 113 cm). Or if linearly extended all the way back to 12 hours, an along-track difference of 5.43 m, implying less than the error caused by using a two-body gravity field, but still perhaps large enough to warrant further investigation.

Result 3 is of interest since the Osculating Cartesian values (i.e. position and velocity) are tangible quantities such that adding the delta-v has a straightforward result. Similarly, the instantaneous Keplerian ellipses associated with the pre- and post-maneuver Cartesian elements, although at the first level of abstraction, are clearly defined. However, what is not as clear is how the difference between those two ellipses translates to the entire orbit, which is better represented by the change in Mean elements. The difference between Results 2 and 3 can be explained by the noting that the argument of latitude at TCA of the maneuver time were 109 and 287 degrees respectively (note Mean and Osculating aol values are very close to each other), thus maneuver time is about 29.4 minutes after the descending node. Therefore, Result 2 corresponds to the black square on Fig. 4 and Result 3 corresponds to the black circle.

A similar analysis with delta-v set to zero indicated that there was a greater error in the Mean/Osculating/Mean conversions than there was in the short-cut vs full methods (Results 1 vs 2). Therefore, the preliminary conclusion for operations is that the short-cut method is better for both computational speed and accuracy. Though note that the accuracy of the MONTE Mean/Osculating conversions can be improved by adjusting the input parameters at the expense of computational speed.

### 3.4 Alternative Mean Element and Maneuver Implementations

#### 3.4.1 Gauss's Equations

An alternative to adding the Δv in Cartesian coordinates was developed by Gauss (adapted from page 184 of Roy's textbook [15] ).

$$\Delta a = 2p * \frac{\Delta v}{n * r\sqrt{1-e^2}}$$

$$\Delta e = \sqrt{1-e^2} * \Delta v * \frac{\cos(E) + \cos(f)}{n * a}$$

$$\Delta \varpi = \sqrt{1-e^2} * \Delta v * \left(1 + \frac{r}{p}\right) * \frac{\sin(f)}{n * a * e}$$

$$\Delta \varepsilon = \frac{e^2}{1 + \sqrt{1-e^2}} * \Delta \varpi$$

where $a$ is semi-major axis, $p$ is semi-latus rectum, $n$ is mean motion, r is radius, e is eccentricity, $\Delta v$ is delta-velocity in the transverse direction, E is eccentric anomaly, f is true anomaly, $\varpi$ is argument of longitude = $\omega + \Omega$, and $\varepsilon$ is the Mean longitude = $\varpi$ + M, where M is the mean anomaly. The proposed idea would be to apply the delta-v to the propagated orbital elements (either Mean or Osculating, see Subsection 3.3.1), producing the $\Delta\alpha$ in Fig. 8 without having to convert to Cartesian. However, an instigation of a State class (python object) in MONTE is stored in Cartesian elements. So in that sense the conversion has already occurred. This could be circumvented with some special coding outside of MONTE, but this effort will be deferred to the future.

## 4. THE AGGREGATE Pc DEBATE

Consider two conjunctions at $TCA_1$ and $TCA_2$ with the two different secondary bodies. A similar discussion can be made for a repeat conjunction with the same secondary though the correlation in the secondary states is greater in that case. The corresponding (no RMM) Pc values are $Pc_1$ and $Pc_2$ and the aggregate Pc is simply modeled as $Pc_1 + Pc_2$. However, when creating the Aggregate Pc plot, an interesting debate has arisen. As can be seen in Fig. 9, the controversy revolves around what should be used for the Pc value for the first conjunctions in the time period between $TCA_1$ and $TCA_2$. Since the time of the MTS plot generation is before $TCA_1$ then the aggregate risk is arguably the inherent risk of not doing an RMM before $TCA_1$ plus the risk from the second object corresponding to any RMM performed in this time period. The counter-argument is that once the $TCA_1$ has passed (successfully!)

then the first conjunction can be ignored and only the risk from the second conjunction should be included (thus corresponding to a Pc = 0 in the blue area of Fig. 9d).

Mathematically speaking the first option is more rigorous though the second option appears to be more practical. Further debate is warranted if the first conjunction's Pc is below the maneuver threshold (standard is $1x10^{-4}$), say $0.9x10^{-4}$ and say the Pc from the second conjunction is $0.8x10^{-4}$. The question is then: has the maneuver threshold been exceeded mandating an RMM before the first conjunction? The discussion then digresses into the relationship between "lifetime risk" and the risk from individual, or in this case conjunctions in quick succession. Such a discussion is going on during peer reviews for new NASA standards.

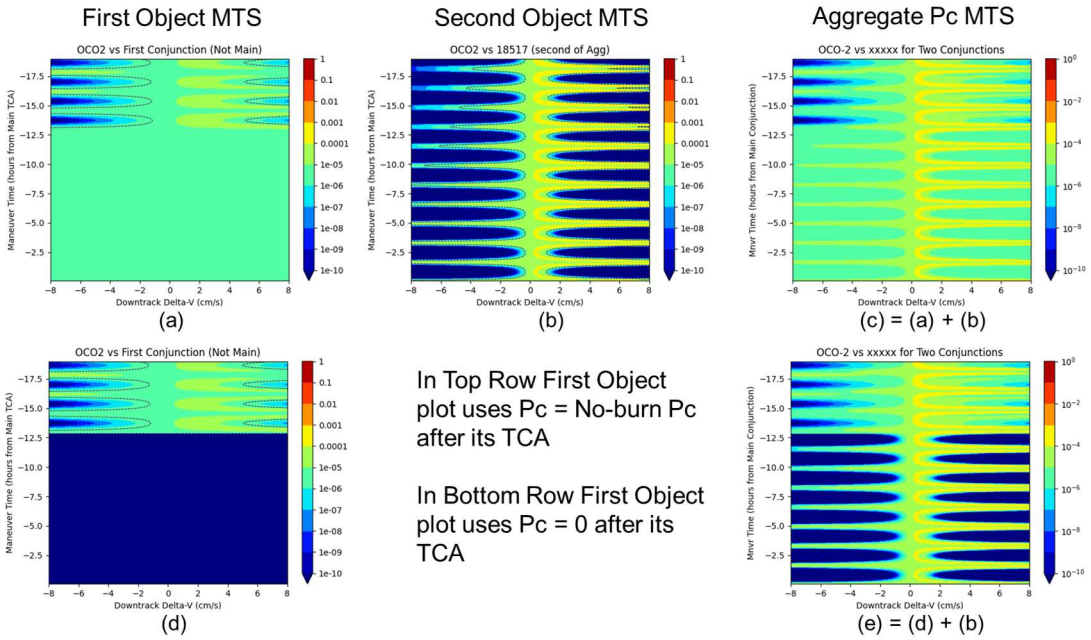


Fig. 9. Aggregate Pc Options

## 5. CONCLUSIONS

With the ultimate goal of reducing the time to create a maneuver Trade Space plot, reducing the force model successfully balances speed and accuracy. In particular, a 4x4 gravity field with no other forces included decreased the computer run time by about a factor of ten while maintaining accuracy good enough for satellite operations. Further investigation is warranted especially for the longer propagations involved in multiple conjunctions with secondary objects. Utilizing Mean element propagations looks promising for decreasing the run times even further, perhaps by another order of magnitude, though this analysis is on-going. The new tools that have been built by JPL were also used to demonstrate an open question about how the Pc from an earlier conjunction is combined with the Pc from a later conjunction in the time period between the two conjunctions.

## 6. ACKNOWLEDGEMENTS

The author would like to thank Aldo Navarro, Ted Sweetser, David Baker and Dan Lyons for reviewing this paper plus Ted Drain, Min-Kun Chung and William Schulze with coding assistance for the MONTE prototypes used to create the results presented here. Thanks also go to Todd Ely for helping to test his Mean element methods for use in this analysis.

## 7. REFERENCES


[1] J.L. Foster and H.S. Estes, "A Parametric Analysis of Orbital Debris Collision Probability and Maneuver Rate for Space Vehicles," NASA JSC 25898, August 1992.

[2] D.T. Hall, "Expected Collision Rates for Tracked Satellites," Journal of Spacecraft and Rockets, Vol.58, No. 3, pp. 715-728, January 31, 2021.

[3] S. Alfano, "Relating Position Uncertainty to Maximum Conjunction Probability," J. Astronautical Sci, Vol. 53, No.2, 2005.

[4] M.A. Vincent, "Bridging the Gap between Academia and Operations for Orbital Debris Risk Mitigation, Proc. of AMOS Conference," Maui, Hawaii, September 15-18, 2015.

[5] T.H. Sweetser, M.A. Vincent & S.J Hatch, "Shootin' the Pipe around the World: Orbit Design and Maintenance for L-Band SAR Radar Interferometry." Proc. of the AIAA/AAS Astrodynamics Specialist Conference, San Diego, CA, August 4-7, 2014.

[6] S. Alfano, "Review of conjunction probability methods for short-term encounters," in Proceedings of the 17th AAS/AIAA Space Flight Mechanics Meeting, Sedona, AZ, Paper AAS-07-148, January 2007.

[7] M.A. Vincent, "Strengthening the bridge between academia and operations for orbital debris risk mitigation," Proc. Of the Advanced Maui Optical and Space Surveillance Technologies Conference, Sept. 19-22, 2017.

[8] R.S. Park and D.J. Scheeres, "Nonlinear Semi-Analytic Methods for Trajectory Estimation," J. of Guidance, Control, and Dynamics, Vol. 30, No. 6, Nov-Dec 2007.

[9] J.H. Kwok, The Long-term Orbiter (LOP), JPL Engineering Memo 312/86-151, June 30, 1986.

[10] J.C. Smith, Planetary Observer Planning Software (POPS), Reference JPL-45418, NASA Technology Transfer Program, also JPL Internal Document EM 312/91-162, February, 1991.

[11] J.R. Guinn, J.R., Periodic Gravitational Perturbations for Conversion between Osculating and Mean Orbit Elements, Advances in Astronautical Sciences, Vol. 76, Specialist Conference, Durango, CO August 19-22, 1991.

[12] W.M. Kaula, *Theory of Satellite Geodesy*, Dover Publications 2000.

[13] T.A. Ely, Mean Element Propagations using Numerical Averaging, Journal of Astronautical Sciences, Vol. 61.3, 2014.

[14] T.A. Ely, Transforming Mean and Osculating Elements using Numerical Methods, Journal of Astronautical Sciences, Vol. 62.1, March 2015.

[15] A. E. Roy, A.E., *Orbital Motion*, Halsted Press, John Wiley and Sons, 1978.